*minerals*

MDPI

*Article*

# Past Hydrological Conditions in a Fluvial Valley: Records from C-O Isotope Signatures of Holocene Sediments in the Loire River (France)

**Philippe Négrel * and Wolfram Kloppmann**

BRGM, F-45060 Orléans, France; w.kloppmann@brgm.fr

* Correspondence: p.negrel@brgm.fr

Received: 26 March 2020; Accepted: 29 April 2020; Published: 29 April 2020


**Abstract:** Multi-proxy indices (grainsize distribution, mineralogy, $\delta^{18}O$, $\delta^{13}C$) in sediments from a meander infill in the Middle Loire alluvial plain of central France are used to highlight some aspects of the basin evolution over the period from 0 to 10,000 years BP. During the Late-Glacial and Holocene period, the lacustrine carbonate substratum of the alluvial plain was incised by the Loire River, creating numerous oxbows and channels related to meander migration. The channel fills consist mainly of fine clayey sediments deposited during flooding of the river, with an almost total absence of coarse-clastic and sandy material, except in the basal part. The record of isotope ratio variations together with the distribution of particle sizes allows the evolution of the river dynamics to be constrained. The strong decrease of carbonate $\delta^{13}C$ in the upper part of the record is ascribed to a progressive closure of the meander and, thus, an increasing control of the C-isotope signature by biological activity in a local environment. Variations in carbonate $\delta^{18}O$, rather, reflect paleohydrological/paleoclimatic changes at the basin scale. The isotope record of the river dynamics also agrees with the variations in clay mineralogy.

**Keywords:** River Loire; Holocene; fluvial dynamics; clay-mineralogy; stable isotopes

## 1. Introduction

Valley floors receive and record part of the erosive flux and act as archives of different types of events at the catchment scale [1–4]. Lithology, relief, climate and human history [5] are the factors that influence erosion rates and catchment input. The composition of sediments in rivers is used for interpreting continental erosion [6]. Additionally, human activities can profoundly modify the sediment yield [5]. Surface streams transport the chemical and mechanical weathering products as sediments, and about 90% of this load is stored in the alluvium for long-terms periods of up to 1000 years [4]. Texture, sedimentary structure and geometry help distinguishing a wide variety of facies and their associations in aggradational sequences. These record the temporal evolution of fluvial, lacustrine and/or palustrine environments that result from aggradation, progradation, retrogradation and lateral-migration processes [1,7].

The present-day mechanisms of trace-elements transfer in the Loire drainage basin (biologically induced calcite and Fe-Mn hydroxides precipitation), were unravelled [8–11] and the evolution of the Middle Loire basin was elucidated [12–14], better constraining the river dynamics. In this study, we present $\delta^{18}O$ and $\delta^{13}C$ data on carbonates, and granulometric and mineralogical proxy indices of the Holocene Loire River dynamics in sediments from a channel infill in the middle Loire alluvial plain. These data highlight some aspects of the basin evolution over the past 10,000 years. Classically, the stable O- and C-isotope ratio variations associated with particle-size distribution patterns allow the evolution of paleo-river or -lake dynamics to be constrained [15–17]. Isotope tracers establish the links

between external drivers (climatic and tectonic evolution, human impact) and river response [18–21], as, due to low burial depths, diagenesis will only slightly alter the signals in river or lake sediments, contrary to many marine environments [22]. Recently, it was demonstrated that carbonate O- and C isotopes from lake sediments or carbonate concretions are in some cases favourable paleo-flood proxies [23] or a climatic record for sub-recent times [24].

## 2. Materials and Methods

### *2.1. Site Description*

The Loire river (117,800 $km^2$) drains central France with a course of more than 1000 km in length (Figure 1, [8]). Palaeozoic granite, gneiss and micaschist (500 to 300 Ma) and a large volcanic area constitute the bedrocks of the upstream section of the catchment. The marine and lacustrine carbonate deposits (200 to 6 Ma) of the Paris Basin constitute the intermediate part of the catchment. The bedrock at the sampling site in the Avaray Valley consists of limestone (Aquitanian lacustrine carbonates; Figure 1, [12]). The site is located at a spot within the global drainage system of the Loire river where 40% of the total catchment is covered.

An oxbow infilling representing a sediment aggradation covering at least 8.5 ka with a sedimentation rate of around 0.6 $mm \cdot a^{-1}$ ([12,25]) was collected for geochemical investigations (cores M25B, M30 and M19, Figure 1). The chronology of the deposits was obtained through 20 radiocarbon dating on the M25B core, 4 on the M19 core, and 1 on the M30 core [14]. In this study, 26 samples were collected from the M25B core, extracted from 6.3 m of Holocene sediments (Table 1), from 0.8 m depth—considered as the lower limit of agricultural reworking—to the bottom of the core. Two further samples were collected from a second core (M30, Figure 1) at a depth of 2.43 m (medium black sand, 11,460 ± 90 a BP, [12]) and at 2.18 m depth (black clay). A sample of Aquitanian lacustrine carbonate was collected from a third core (M19) at 5 m depth. The description of the M25B core is as follows: (a) to (i) referring to identified units with $^{14}C$ dating [12]; see also Figure 2. The evolution along the core is a classical sequence corresponding to a channel migration from the base of the channel to a more riparian environment.

(i) lower part (interval 6.3–4.9 m) of the core consists of coarse- and fine-to-medium grained micaceous sand;
(h) 4.9–4.7 m: very fine black peat, the base is dated 8410 ± 70 a BP;
(g) 4.7–3.5 m: black peat, becoming brownish towards the top, containing ligneous debris and gastropods (6840 ± 70 a BP at 3.58 m);
(f) 3.5–2.9 m: black clay, rich in well-preserved gastropods, with ligneous debris dated as Atlantic;
(e) 2.9–2.7 m: black clay with sparse gastropods and wood fragments (5350 ± 60 a BP at 2.77 m, end of Atlantic);
(d) 2.7–2.2 m: grey to green clay, sparse shelly debris and very rare vegetal debris (Atlantic);
(c) 2.2–1.0 m: compact green clay with blue spots and sparse gastropod debris (3360 ± 50 a BP at 2.16 m depth; Subboreal 2370 ± 50 a BP at 1.65 m depth, Subatlantic);
(b) 1.0–0.9 m: brownish clay grading into loamy clay;
(a) 0.9–0 m: brown clayey loam and soil.

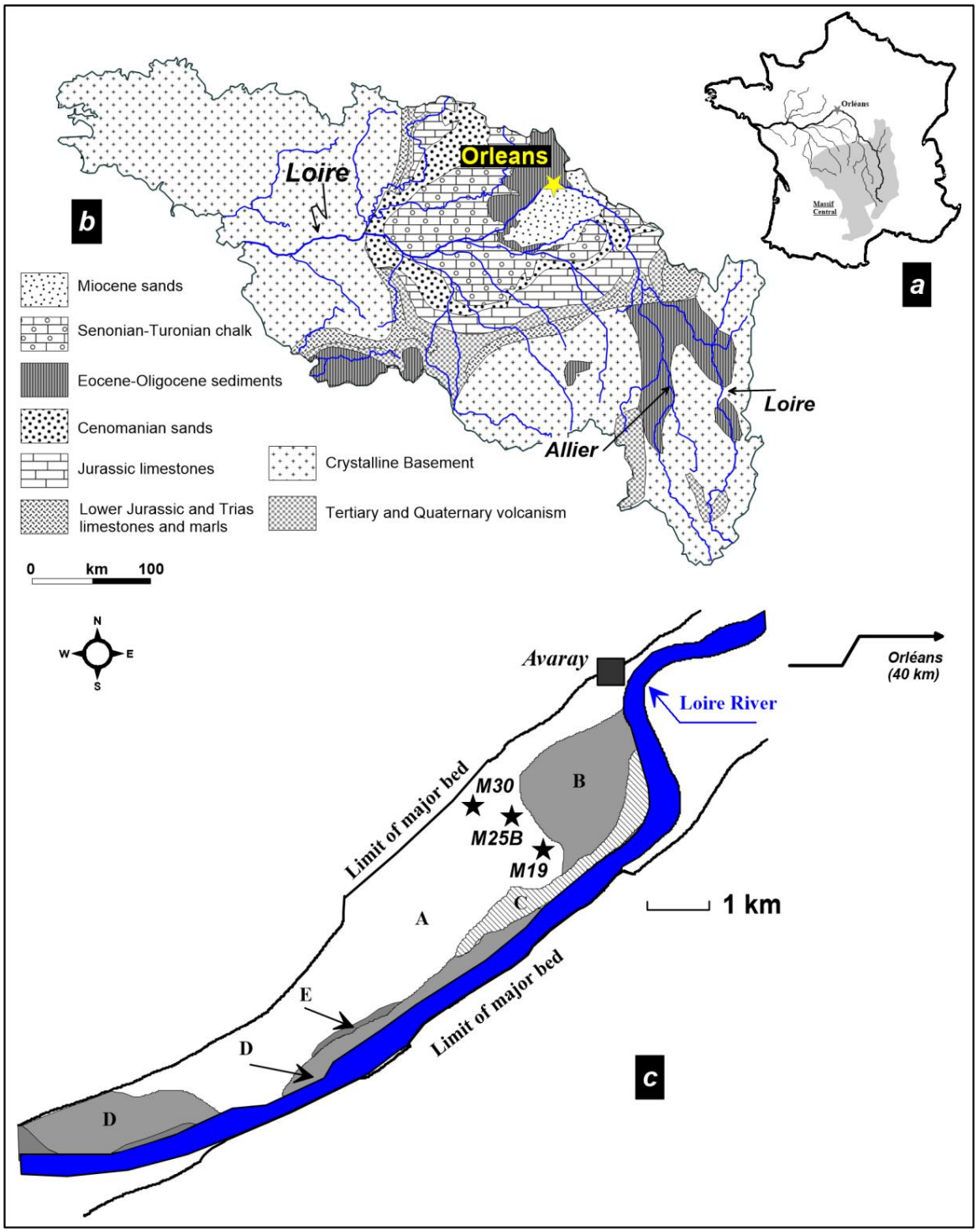


**Figure 1.** (**a**) Location of the Loire River catchment in France. (**b**) Simplified geological map of the upper Loire river catchment (modified from Négrel et al. [9]); (**c**) map of the Val d'Avaray meander. The sites where the cores were extracted are indicated, the meander structure and distribution of sediment bodies A–E (modified from Garcin et al. [12]) are also shown. The bodies were identified on the basis of aerial photographs, lithological data, thickness and altitude of the Aquitanian limestone substratum provided by more than 200 boreholes in the area. Each body corresponds to a slight migration of the main river channel. Stage A is the oldest, corresponding to migration of a meander with frontal erosion and prograding sand bars, and was eroded by stage B. Bodies C and D have a slightly sinuous to rectilinear path and body E shows well-preserved sand-filled channels and islands.

### *2.2. Sample Pretreatment and Methods*

After drying, each sample was homogenized by hand-crushing in an agate mortar.

The mineralogical composition of the sediment sample was determined by X-ray diffraction (XRD) according to the procedure given by Négrel and Grosbois [8] and reference therein. Each bulk sample was homogenized by hand-crushing with an agate mortar. A mix of 5 mg of powder and 3 mL of distilled water were placed on glass slides and air dried for 3 h. The mineralogical composition was determined by X-ray diffraction using a Rigaku analyser, Cu-$K_\alpha$ ray with a Ni-$K_\beta$ filter and diffraction spectra allowing the qualitative mineralogical composition to be defined. For each mineral, the ratio of the height of its most intense peak against the sum of all the most intense mineral peaks was used to calculate the semi-quantitative percentages [10].

The C and O isotopic ratios of the carbonate and bulk samples were analysed with a Finnigan MAT 252 mass spectrometer connected to an automatic carbonate-preparation Kiel device. They were reported in per-mil deviations from the international V-PDB standard with an average precision, based on replicate analyses of various samples and laboratory standards, of ±0.1‰ for $\delta^{18}O$ and $\delta^{13}C$ (2σ; [9]). Gastropod shells were analysed after cleaning with distilled water and hand crushed for C and O isotopic ratios with the Finnigan MAT 252 mass spectrometer following manual preparation of the sample.

## 3. Results and Discussion

### *3.1. Clay Mineralogical Changes in the Loire River Reflecting Weathering Intensity*

The channel fill consists of fine clayey overbank deposits corresponding to flooding of the river, as shown by the variation in the particle sizes (Figure 2a). The particle sizes and the semi-quantitative XRD analysis of the sediment showed that clay minerals constitute between 25% and 90% of the sediment (Table 1, Figure 2b). Quartz, feldspar and calcite range from less than 5% to 40%. The particle-size distribution is given in Figure 2a (Fμm stands for the fraction expressed in μm). It shows a total absence of coarse clastics and sand in the core, except in lowest part (±10% at 3 to 3.75 m depth). Particles in the range 20 < Fμm < 63 gently decrease upward in the core from 30% to around 20%. Particles with a size of up to 20 μm represent a mean of 76 ± 14% in the channel fill, separated in two fractions (4 < Fμm< 20 and Fμm < 4). The 4 < Fμm <20 fraction increases steadily upward from 20% at the base up to 40% at the top of the channel fill, whereas the Fμm <4 fraction remains relatively constant around 40% in the core.

The <4 μm fraction (Figure 2b) is dominated by mixed layer minerals illite/smectite (30%–90%), illite, illite/chlorite, chlorite and kaolinite making up the rest of the clay minerals. The distribution of the clays shows an up-core increase in illite/smectite and, conversely, a decrease in kaolinite and illite abundance. The increase of the illite/smectite abundance is large, starting around 25% at 4.75 m depth to reach over 85% at the top of the channel fill. Figure 2b shows the relative individual clay mineral contents compared to total clay content in the sample. This normalization allows excluding effects that might originate from changes in the depositional environment such as sudden changes in transport velocity. The clay minerals in soil are the result of weathering processes in the parent rocks [26,27]. It is generally agreed that the differences in clay-mineral composition in soil or in river sediments reflect weathering intensity [17] as well as weathering mechanisms (i.e., physical vs. chemical weathering). Clay mineral genesis reflects climatic variations, of both precipitation and temperature, and the lithological and morphological settings [28].

The weathering types and their intensity, at the basin scale, can be estimated from the clay minerals in riverine sediments [29] when comparing the conditions of formation of each clay type [30]. Kaolinite is formed by intensive hydrolysis in a warm and humid climate. Illite and chlorite are formed by weak hydrolysis and/or strong physical erosion of bedrock in a relatively dry climate, being primary minerals of weathering processes. Smectite formation in soil requires a warm and wet climate with

poor drainage. Illite/chlorite also indicate the nature of the weathered bedrock, being more abundant during the weathering of felsic rather than mafic rocks [30].

The clay-mineral assemblages of sediments help to constrain their sources and transport pathways, and provide information about the related paleoenvironmental and paleoclimatic conditions. For this purpose, a ternary diagram of the clay-mineral groups illite+chlorite, kaolinite, and smectite (Figure 3; [31]) illustrates the three parameters of sources, processes and pathways in the channel fill. As mentioned above, kaolinite is formed by chemical weathering, while illite/chlorite are mostly inherited from parent rocks by physical erosion. Thus, the kaolinite vs. illite/chlorite ratio indicates the types of weathering (chemical weathering vs. physical erosion) that affected the sediments, with the weathering intensity given by smectite.

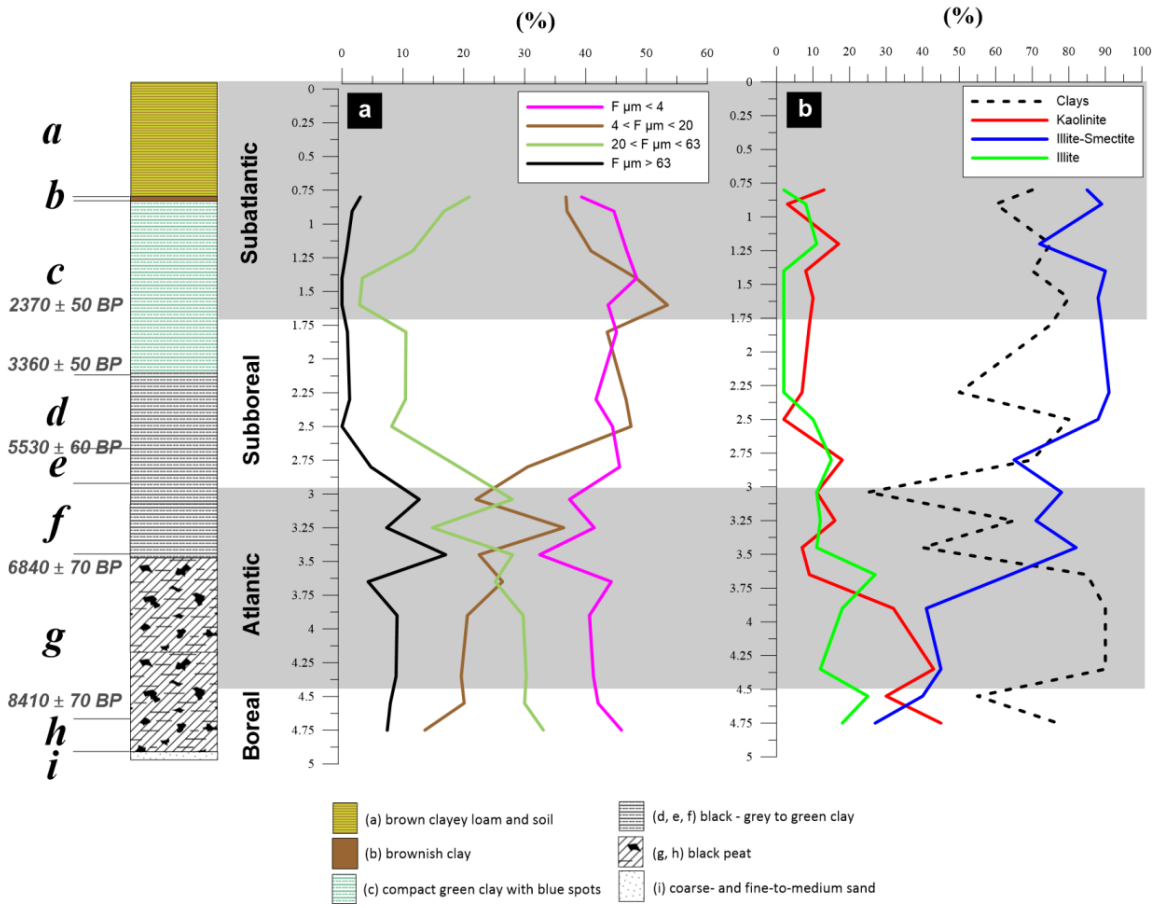


**Figure 2.** Variations of particle size (%, **a**) and clay content (%, **b**) in the M25B core. Radiocarbon dates are from [12], see Table 1 for more details and text for the location of the $^{14}C$ dates.

**Table 1.** Semi-quantitative X-ray diffraction (XRD) analysis of the sediment in the M25B core. Radiocarbon dates are issued from the interpretation given by [12].

| Sample | Z | Age | Quartz | Feldspaths | Calcite | Phyllosilicates | Smectite-Illite | Illite | Kaolinite | Chlorite | Illite-Chlorite |
|---|---|---|---|---|---|---|---|---|---|---|---|
| | m | a BP | % | % | % | % | % | % | % | % | % |
| M25B/A | 0.80 | 1137 | 15 | 15 | | 70 | 85 | 2 | 13 | | 2 |
| M25B/B | 0.91 | 1309 | 15 | 25 | | 60 | 89 | 8 | 3 | | 8 |
| M25B/C | 1.20 | 1791 | 10 | 10 | 5 | 75 | 72 | 11 | 17 | | 11 |
| M25B/D | 1.40 | 2117 | 10 | 15 | 5 | 70 | 90 | 2 | 8 | | 2 |
| M25B/E | 1.60 | 2444 | 10 | 5 | 5 | 80 | 88 | 2 | 10 | | 2 |
| M25B/F | 1.80 | 2771 | 12 | 10 | 3 | 75 | 89 | 2 | 9 | | 2 |
| M25B/G | 2.30 | 3587 | 5 | 10 | 35 | 50 | 91 | 2 | 7 | | 2 |
| M25B/H | 2.50 | 3914 | 5 | 5 | 10 | 80 | 88 | 10 | 2 | | 10 |
| M25B/I | 2.80 | 4404 | 5 | 5 | 20 | 70 | 65 | 15 | 18 | 2 | 17 |
| M25B/J | 3.04 | 4796 | 5 | 30 | 40 | 25 | 78 | 11 | 11 | | 11 |
| M25B/K | 3.25 | 5139 | 15 | 10 | 10 | 65 | 71 | 12 | 16 | 1 | 13 |
| M25B/L | 3.45 | 5466 | 5 | 15 | 40 | 40 | 82 | 11 | 7 | | 11 |
| M25B/M | 3.65 | 6831 | 5 | 10 | | 85 | 64 | 27 | 9 | | 27 |
| M25B/N | 3.90 | 7202 | 5 | 5 | | 90 | 41 | 18 | 32 | 9 | 27 |
| M25B/O | 4.35 | 7870 | 5 | 5 | | 90 | 45 | 12 | 43 | 0.1 | 12 |
| M25B/P | 4.55 | 8166 | 3 | 2 | 40 | 55 | 40 | 25 | 30 | 5 | 30 |
| M25B/Q | 4.75 | 8463 | 3 | 5 | 15 | 77 | 27 | 18 | 45 | 10 | 28 |

In Figure 3, the smectite values increase along the blue arrow, defining an up-core trend that suggests a less intense chemical weathering and a weak physical erosion for the younger sediments, and a more mafic (more basalt weathering) than felsic source for the clay-mineral origin.

These results give an insight into the changes that affected the Loire basin over the past 8500 years, and most likely indicate the dispersal of fine sediments during the yearly floods of the river. Over the same period, the weathering of basalt in the Massif Central has increased, as shown by lead isotopes [14], while granite weathering has decreased. The authors demonstrate [14] that the lead isotope has recorded the volcanic events (Vasset/Killian tephra event, 8300 BP) and also the increase of the erosion processes of volcanic material through soil cultivation in the mid to late Holocene. The decrease in physical erosion has favoured a relative increase in the importance of chemical weathering, agreeing with the gently up-core decrease of the 20 < Fμm < 63 fraction and the increase in the 4 < Fμm < 20 fraction, the latter being more easily transported by the river in terms of velocity capacities. This is also marked by a stability of the Fμm < 4 fraction in the channel fill as a mark of the final filling steps.

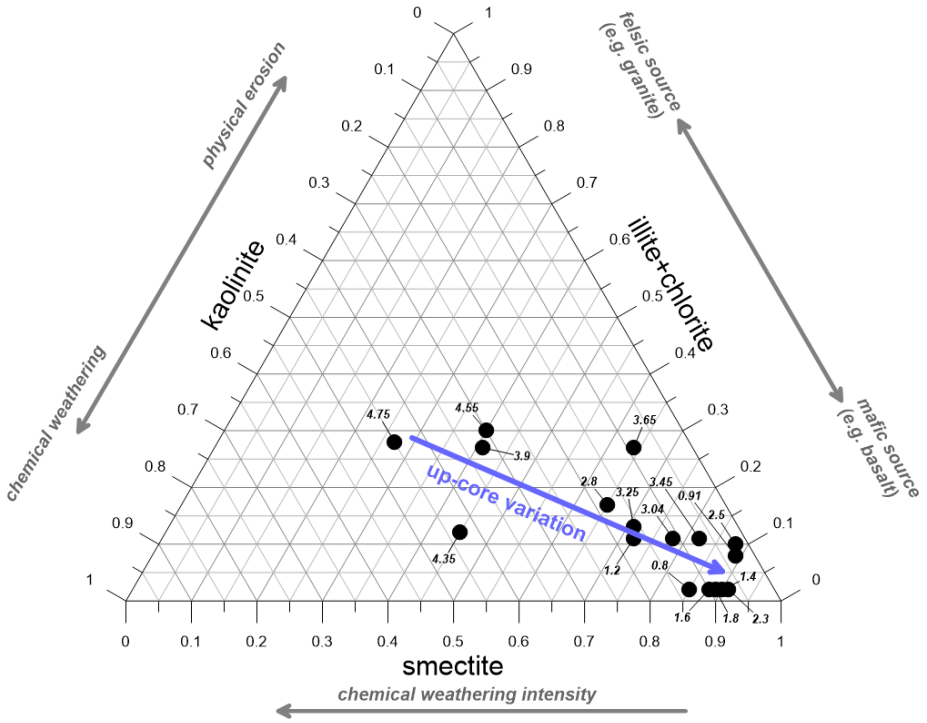


**Figure 3.** Ternary diagram of the major clay-mineral groups illite-chlorite, kaolinite, and smectite [31]. This clay-mineral assemblage reflects both source-rock lithology and past climate. Kaolinite and smectite abundances are proxies for weathering intensity, whereas the illite-chlorite abundance depends upon the lithology of source rocks.

### *3.2. Origin of Carbonate in the Flood Sediments*

The study by Négrel et al. [13] on this channel infill suggests that the carbonates in the sediment record are authigenic rather than detrital in origin. Additionally, carbon- and oxygen-isotope compositions of fluvial and associated carbonate deposits provide environmental information on past temperature, humidity, soil and vegetation, as well as information on the $CO_2$ source in carbonates—thus characterizing catchment areas—and on hydrological and physical features of underground and surface-water systems. A wide range of $\delta^{13}C$ values and a narrower range in $\delta^{18}O$ ones are commonly observed (Table 2). A narrower range in $\delta^{18}O$ because carbonate deposits record variations in $\delta^{18}O$ related to seasonal to decadal temperature changes, which generally are not parallel to $\delta^{13}C$ variations

that may integrate the role of aquatic vegetation as well as early diagenetic reactions during bacterial organic matter degradation [18].

**Table 2.** Carbon- and oxygen-isotope compositions of the sediment in the M25B and M30 cores; Z indicates the sampling below the soil surface.

| Sample | Z | age | $\delta^{18}O$ | $\delta^{13}C$ |
|---|---|---|---|---|
| | m | a BP | ‰ vs. V-PDB | ‰ vs. V-PDB |
| ***M25B core*** | | | | |
| M25B/A | 0.80 | 1137 | −4.2 | −13.3 |
| M25B/B | 0.91 | 1309 | −4.3 | −12.8 |
| M25B/C | 1.20 | 1791 | −2.6 | −12.3 |
| M25B/Ca | 1.30 | 1954 | −4.2 | −10.7 |
| M25B/D | 1.40 | 2117 | −2.8 | −11.3 |
| M25B/E | 1.60 | 2444 | −2.7 | −9 |
| M25B/F | 1.80 | 2771 | −3.5 | −9.1 |
| M25B/Fa | 1.91 | 2950 | −2.6 | −7.8 |
| M25B/G | 2.30 | 3587 | −5.3 | −6.9 |
| M25B/Ga | 2.41 | 3759 | −5.2 | −7.3 |
| M25B/H | 2.50 | 3914 | −4.7 | −8.7 |
| M25B/Ha | 2.70 | 4241 | −4.4 | −7.1 |
| M25B/I | 2.80 | 4404 | −6.7 | −6.5 |
| M25B/J | 3.04 | 4796 | −7 | −6.9 |
| M25B/K | 3.25 | 5139 | −5.7 | −6.9 |
| M25B/L | 3.45 | 5466 | −6.9 | −6.8 |
| M25B/Na | 4.25 | 7721 | −1.4 | −6.8 |
| M25B/O | 4.35 | 7870 | −3.5 | −6.1 |
| M25B/P | 4.55 | 8166 | −6.4 | −6.1 |
| M25B/Pa | 4.65 | 8315 | −6.1 | −5.6 |
| M25B/Q | 4.75 | 8463 | −4.1 | −5.5 |
| ***M30B core*** | | | | |
| M30A | 2.43 | 11,460 | −6.3 | −5.6 |
| M30B | 2.18 | - | −6.8 | −4.9 |
| ***Aquitanian carbonate*** | | | | |
| M19/5 | 5.00 | - | −2.4 | −5.7 |
| ***gastropod shells*** | | | | |
| M25B/Ds | 1.40 | - | −4.5 | −10.1 |
| M25B/Gs | 2.30 | - | −4.5 | −10.2 |
| M25B/Ks | 3.25 | - | −5.7 | −9.6 |
| M25B/Ls | 3.45 | - | −5.6 | −12.5 |

The range of δ values is wide for both $\delta^{18}O$ (~−7.0‰ to −1.4‰) and $\delta^{13}C$ (~−13.3‰ to −5.5‰). The stable-isotope record in Figure 4 shows several remarkable features: (1) From 0.75 m to 2.3 m $\delta^{13}C$ strongly increases from −13.3‰ to −6.9‰ and then stabilises around −6‰; (2) The interval (4.55–3.45 m) is marked by a positive peak of $\delta^{18}O$ values; (3) From 3.04 m upwards, the $\delta^{18}O$ values evolve towards higher values. For the gastropod shells, analysed when they could be isolated from the rest of the sediment, the $\delta^{18}O$ values more or less agree with those observed in the sediment, suggesting equilibrium both for carbonate precipitation in the sediment and in the organisms colonizing the meander. However, the $\delta^{13}C$ in gastropod shells only matches the sediment carbonates at 1.40 m depth in the channel fill, the three other gastropod samples are depleted in $^{13}C$ by 2.7‰ to 5.7‰ compared to the sediment $\delta^{13}C$. Similar depletions in $^{13}C$ compared to equilibrium values (by 1‰ to 4‰) have been observed for certain species of freshwater gastropods, mainly lung-breathing, pulmonate gastropods, whereas gill-breathing species are close to equilibrium with dissolved inorganic carbon DIC [32], highlighting the limitations for interpreting stable isotopic data from fossil gastropod shells.

Négrel et al. [9] investigated the carbonate fraction of present-day suspended matter in the Loire River with stable carbon- and oxygen-isotope compositions (Figure 4). The recorded values varied from −3.1‰ to −7.6‰ for $\delta^{13}C$ and from −1.7‰ to −9.4‰ for $\delta^{18}O$. The relationship between $\delta^{18}O$ and $\delta^{13}C$ (Figure 4) indicates that "winter" carbonate sampled during high-flow conditions is clearly different from "summer" carbonate sampled during low-flow conditions. The latter occupies a restricted area with $\delta^{13}C = -7‰$ and $\delta^{18}O = -8‰$. The $^{18}O$ content of the water and the $^{13}C$ content of the total DIC and their variations during changes of environmental conditions directly impact the isotope contents of authigenic carbonate. Calcite precipitation during low flow is in isotopic equilibrium with DIC which is derived in different proportions from atmospheric $CO_2$, dissolved carbonates and from biogenic $CO_2$ produced during degradation of organic matter. During high flow, the relative contribution of atmospheric $CO_2$ and/or of erosive carbonates increases.

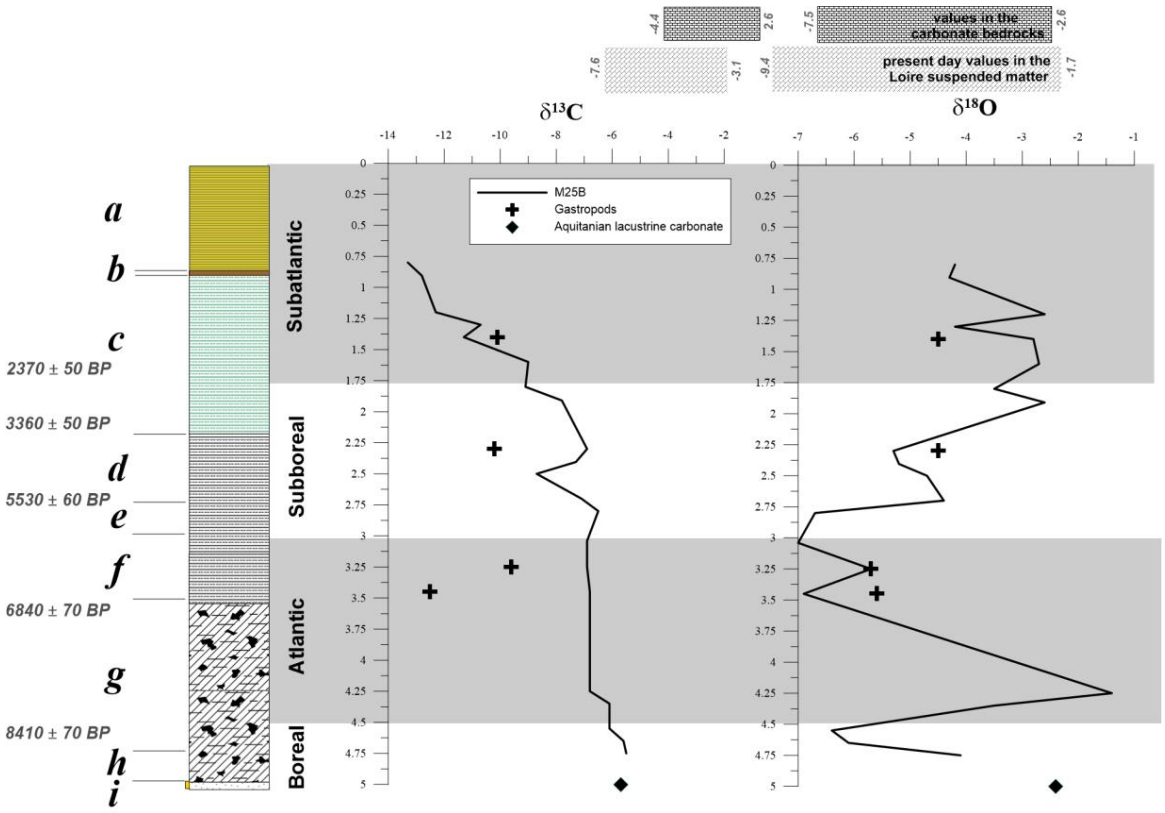


**Figure 4.** The Loire stable-isotope record: $\delta^{18}O$ and $\delta^{13}C$ values for the carbonate fraction and gastropod shells. The carbonate fraction of present-day suspended matter in the Loire River over a one-year cycle, and six representative rock samples were analysed for their stable-isotope contents by Négrel et al. [9]. Legend of the sedimentary deposits as in Figure 2.

Fontes et al. [15] listed the factors that can control the evolution of $\delta^{18}O$ and $\delta^{13}C$ values in authigenic carbonate in lakes, which can be transposed to rivers. An increase in the $\delta^{18}O$ values of authigenic carbonate may be due to: (1) enrichment of the heavy isotope in rain inputs (origin, type of condensation of air moisture, lower relative humidity); (2) increase in the average water temperature; (3) a longer residence time of the water in the water body (notably lakes) and/or lower relative humidity enhancing evaporative enrichment in heavy isotopes.

A decrease in the $^{13}C$ content of authigenic carbonates may be due to: (1) a lower isotope exchange of the total DIC with atmospheric $CO_2$ through a shorter residence time of the water; (2) growth of vegetation cover in the catchment or in the vicinity of the site, (e.g., a riparian forest as last step in channel migration) and concomitant oxidation of organic matter; (3) an increase in partial pressure

of soil $CO_2$ in the catchment area or in the vicinity of the site, leading to a lower $^{13}C$ content in the total DIC.

The observed opposing trends in the upper part of the channel fill, from the Subboreal onwards, can be due to several causes, dependent or independent of the hydrological behaviour in the meander [33]. The rapid throughflow in the Loire River system implies that the $^{18}O$ content of water reflects the mean composition of precipitation at the catchment scale. Therefore, the $^{18}O$ variations of carbonates give a clue on the composition and patterns of regional precipitation as well as on the effect of the water temperature as evidenced in present-day suspended matter [18]. Additionally, such rapid throughflow also precludes causing an exchange of the total DIC with atmospheric $CO_2$ for the $^{13}C$ variations. To illustrate the opposite, but concomitant, variations in $^{18}O$ and $^{13}C$ contents, we plotted such data in a $\delta^{18}O$ vs. $\delta^{13}C$ diagram (Figure 5). There is no clear overall trend between $\delta^{18}O$ and $\delta^{13}C$ values, but it is worth noting that (1) the deeper samples agree with the range seen in the carbonate fraction of present-day suspended matter in the Loire River, and that (2) around 2.5–2.4 m depth a large decrease is seen in $\delta^{13}C$, which occurred around 4400 a BP. This decrease is accompanied by a smaller variation of the $\delta^{18}O$ value.

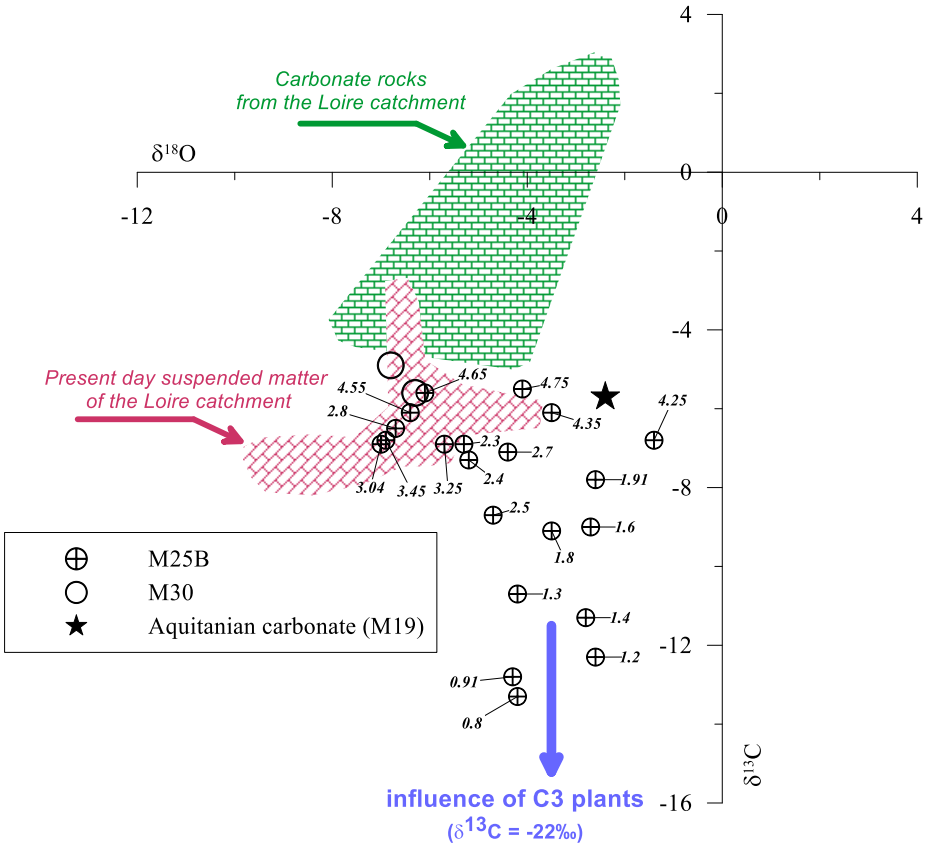


**Figure 5.** Isotopic compositions $\delta^{18}O$ vs. $\delta^{13}C$ of authigenic carbonates of the Loire channel fill. The carbonate fraction of present-day suspended matter in the Loire River over a one-year cycle, and six representative rock samples were analysed for their stable-isotope contents by Négrel et al. [9] and are shown in red and green, respectively. Numbers indicate the depth of the samples in the channel fill.

The plants that colonized the meander are expected to be predominantly C3 so that sedimentary $\delta^{13}C$ variations cannot be explained by a change in the relative proportions of C3 and C4 plants. Native C4 plants currently make up only 1.05% of the plant species in France [34] and during colder periods, this proportion would even have been less. Any significant contribution of C4 plants to the overall soil organic C budget would not be expected before the massive introduction of maize in the 20th century. Even though, the opposing $\delta^{13}C$ and $\delta^{18}O$ trends can be ascribed to a progressive closure of

the meander and the installation of C3 vegetation. This newly created non-permanent wetland [35] was regularly destroyed by river floods during the winter months and by stagnant water in the meander. Thus, the C isotope signature was mainly controlled by a local environment with more negative $\delta^{13}C$ values due to the oxidation of plant debris. This bacterially driven organic-matter mineralization means that organic C, with metabolic products, are released into the porewater, and nutrients are transformed into inorganic forms, allowing C to be fixed in authigenic carbonate.

Increasing contribution of local groundwater, dominated by carbonate dissolution would also contribute $^{13}C$-depleted DIC, with a roughly equivalent contribution of biogenic carbon from C3 ($< -26‰$) and the palustrine rock carbonates of the Beauce aquifer ($<0‰$).

High $\delta^{18}O$ values reflect a period of long residence time, induced by evaporation attributed to closure of the meander; this longer water-residence time conferred its signature to the carbonate and was less dependent of the meander evolution. Temperature variations explain most likely the high $\delta^{18}O$ episode during the Atlantic. Whereas the $\delta^{18}O$ value of authigenic carbonates decreases with increasing equilibrium temperature [9,18], this effect can be overridden by long-term temperature effects on the precipitation [18]. The observed positive shift by 5‰ in our study is similar to that observed by Mayer and Schwark [18] in lake sediments in SW Germany at the end of the Boreal (from around −6‰ to −2‰), reflecting the temperature-driven changes in the $\delta^{18}O$ value of rainfall at the basin scale, superposed to other effects, notably evaporation.

## 4. Conclusions

The stable O- and C-isotope ratio variations, the distribution of particle sizes and clay-mineral types, reflect the evolution of river dynamics. Our comprehensive study of a channel-fill system in the Middle Loire alluvial plain suggests that:

(1) The kaolinite vs. illite/chlorite ratio indicates the importance of chemical weathering vs. physical erosion that affected the sediments, with smectite content as weathering intensity proxy. Their variations might reflect a less-intense chemical weathering and a weak physical erosion in the case of the younger sediments, and a more mafic (basalt) than felsic source for the clay-mineral origin, likely related to the increase in the soil cultivation in the mid to late Holocene and a higher contribution of volcanic material to the alluvial deposits [14].

(2) Variations of carbon and oxygen isotopes ratios over the last 10,000 years reveal a wide range. The Atlantic climatic optimum is reflected by a positive $\delta^{18}O$ shift. The opposite trends for $\delta^{13}C$ and $\delta^{18}O$ values observed in the Subboreal and the Subatlantic variations is ascribed to a progressive closure of the meander and the installation of vegetation in a non-permanent wetland. The closure is consistent with the decrease in particle size and reflects the progressive disconnection of the meander with its bed infill, changes in the C origin, and possible difference in oxygen availability affecting the degradation processes of organic matter.

The results of the present study complete previous interpretations, at the local and basin scales, and are consistent with observations from Sr and Pb isotopes [13,14]. A different functioning of the past channels compared to present day conditions was shown by Sr isotopes [13], highlighting the role of local groundwater in the precipitation of authigenic carbonates in the meander. The Pb-isotope variation was related to natural input from erosion and to human impact (mining and smelting of Pb ore, agricultural development impacting the forest) during the past 10,000 years [14]. The isotopic tools complement each other perfectly with a vision that stretches from the global basin scale with Pb and, partly, O-isotopes, down to the very local scale of a meander with Sr and stable O- and C isotopes. Our results prove an unambiguous isotopic imprint of a low-magnitude physical event (closure of the meander over a period of at least 2600 years) in the fluvial sedimentary record. Stable-isotope data are thus a meaningful complement to classic proxies (particle size, clay minerals); they have great potential in the reconstruction of the geomorphological evolution of rivers and are applicable to all streams and lakes with a known sedimentary record.

**Author Contributions:** Conceptualization, methodology, investigation, P.N., W.K.; writing—original draft preparation, P.N.; writing—review and editing, W.K.; All authors have read and agreed to the published version of the manuscript.

**Funding:** This research received no external funding. This work was financially supported by the BRGM Research Program.

**Acknowledgments:** Isotopic analyses benefited from the collaboration of C. Fléhoc in the BRGM isotope laboratories. H.M. Kluijver edited the manuscript and proofread the English.

**Conflicts of Interest:** The authors declare no conflict of interest.

## References

1. Meade, R.H. Movement and storage of sediment in river systems. In *Physical and Chemical Weathering in Geochemical Cycles*; Lerman, A., Meybeck, M., Eds.; Kluwer Academic Pub: Dordrecht, The Netherlands, 1988; pp. 165–180.
2. Runge, J. Holocene landscape history and palaeohydrology evidenced by stable carbon isotope ($\delta^{13}C$) analysis of alluvial sediments in the Mbari valley (5°N/23°E), Central African Republic. *Catena* **2002**, *48*, 67–87. [CrossRef]
3. May, D.W. Properties of a 5500-year-old flood-plain in the Loup River Basin, Nebraska. *Geomorphology* **2003**, *56*, 243–254. [CrossRef]
4. Dhivert, E.; Grosbois, C.; Rodrigues, S.; Desmet, M. Influence of fluvial environments on sediment archiving processes and temporal pollutant dynamics (Upper Loire River, France). *Sci. Tot. Environ.* **2015**, *505*, 121–136. [CrossRef] [PubMed]
5. Meade, R.H.; Yuzyk, T.R.; Day, T.J. Movement and storage of sediment in rivers of the United States and Canada. In *The Geology of North America, Surface Water Hydrology*; Geological Society of America: Boulder, CO, USA, 1990; pp. 255–280.
6. Gaillardet, J.; Dupré, B.; Allègre, C.J. Geochemistry of large river suspended sediments: Silicate weathering or recycling tracer? *Geochim. Cosmochim. Acta* **1999**, *63*, 4037–4051. [CrossRef]
7. Benito, G.; Sopena, A.; Sanchez-Moya, Y.; Machado, M.J.; Pérez-Gonzalez, A. Palaeoflood record of the Tagus River (Central Spain) during the Late Pleistocene and Holocene. *Quart. Sci. Rev.* **2003**, *22*, 1737–1756. [CrossRef]
8. Négrel, P.; Grosbois, C. Changes in chemical and $^{87}Sr/^{86}Sr$ signature distribution patterns of suspended matter and bed sediments in the upper Loire River basin (France). *Chem. Geol.* **1999**, *156*, 231–249. [CrossRef]
9. Négrel, P.; Grosbois, C.; Kloppmann, W. The labile fraction of suspended matter in the Loire River (France): Multi-element chemistry and isotopic (Rb-Sr and C-O) systematics. *Chem. Geol.* **2000**, *166*, 271–285. [CrossRef]
10. Grosbois, C.; Négrel Ph Grimaud, D.; Fouillac, C. An overview of dissolved and suspended matter fluxes in the Loire River basin: Natural and anthropogenic inputs. *Aquat. Geochem.* **2001**, *7*, 81–105. [CrossRef]
11. Négrel, P.; Roy, S. Investigating the sources of the labile fraction in sediments from silicate-drained rocks using trace elements, and strontium and lead isotopes. *Sci. Total Environ.* **2002**, *298*, 163–182. [CrossRef]
12. Garcin, M.; Giot, D.; Farjanel, G.; Gourry, J.C.; Kloppmann, W.; Négrel, P. Géométrie et âge des alluvions du lit majeur de la Loire moyenne, exemple du val d'Avaray (Loir-et-Cher, France). *Comptes Rendus Acad. Sci.* **1999**, *329*, 405–412. [CrossRef]
13. Négrel, P.; Kloppmann, W.; Garcin, M.; Giot, D. Strontium isotopic record of signatures of Holocene fluvial sediments in the Loire valley, France. *Hydrol. Earth Syst. Sci.* **2002**, *6*, 849–858. [CrossRef]
14. Négrel, P.; Kloppmann, W.; Garcin, M.; Giot, D. Lead isotope signatures of Holocene fluvial sediments from the Loire River valley. *Appl. Geochem.* **2004**, *19*, 957–972. [CrossRef]
15. Fontes, J.C.; Gasse, F.; Gibert, E. Holocene environmental changes in Lake Bangong basin (Western Tibet). Part 1: Chronology and stable isotopes of carbonates of a Holocene lacustrine core. *Palaeogeogr. Palaeoclimatol. Palaeoecol.* **1996**, *120*, 25–47. [CrossRef]
16. Makhnach, N.; Zemitskaja, V.; Kolosov, I.; Simakova, G. Stable oxygen and carbon isotopes in Late Glacial-Holocene freshwater carbonates from Belarus and their palaeoclimatic implications. *Palaeogeogr. Palaeoclimatol. Palaeoecol.* **2004**, *209*, 73–102. [CrossRef]

17. Garzanti, E.; Padoan, M.; Setti, M.; López-Galindo, A.; Villa, I.M. Provenance versus weathering control on the composition of tropical river mud (southern Africa). *Chem. Geol.* **2014**, *366*, 61–74. [CrossRef]
18. Mayer, B.; Schwark, L. A 15,000-year stable isotope record from sediments of lake Steisslingen, Southwest Germany. *Chem. Geol.* **1999**, *161*, 315–337. [CrossRef]
19. Lojen, S.; Dolenec, T.; Vokal, B.; Cukrov, N.; Mihelcic, G.; Papesch, W. C and O stable isotope variability in recent freshwater carbonates (River Krha, Croatia). *Sedimentology* **2004**, *51*, 361–375. [CrossRef]
20. Schulte, P.; van Geldern, R.; Freitag, H.; Karim, A.; Négrel Ph Petelet-Giraud, E.; Probst, A.; Probst, J.L.; Telmer, K.; Veizer, J.; Barth, J.A.C. Applications of stable water and carbon isotopes in watershed research: Weathering, carbon cycling, and water balances. *Earth Sci. Rev.* **2011**, *109*, 20–31. [CrossRef]
21. Parrish, J.T.; Hyland, E.G.; Chan, M.A.; Hasiotis, S.T. Stable and clumped isotopes in desert carbonate spring and lake deposits reveal palaeohydrology: A case study of the Lower Jurassic Navajo Sandstone, south-western USA. *Sedimentology* **2019**, *66*, 32–52. [CrossRef]
22. Reis, A.; Erhardt, A.M.; McGlue, M.M.; Waite, L. Evaluating the effects of diagenesis on the $\delta^{13}C$ and $\delta^{18}O$ compositions of carbonates in a mud-rich depositional environment: A case study from the Midland Basin, USA. *Chem. Geol.* **2019**, *524*, 196–212. [CrossRef]
23. Kämpf, L.; Plessen, B.; Lauterbach, S.; Nantke, C.; Meyer, H.; Chapligin, B.; Brauer, A. Stable oxygen and carbon isotopes of carbonates in lake sediments as a paleoflood proxy. *Geology* **2019**, *48*, 3–7. [CrossRef]
24. Benjelloun, Y.; Carlut, J.; Hélie, J.F.; Chazot, G.; Le Callonnec, L. Geochemical study of carbonate concretions from the aqueduct of Nîmes (southern France): A climatic record for the first centuries AD? *Sci. Rep.* **2019**, *9*, 5209. [CrossRef] [PubMed]
25. Garcin, M.; Giot, D.; Farjanel, G. Radiocarbon dating and palynology of alluvial deposits in the Loire flood plain (Val d'Avaray, Loir et Cher, France). *Quaternaire* **2001**, *12*, 69–88. [CrossRef]
26. Wilson, M. The origin and formation of clay minerals in soils: Past, present and future perspectives. *Clay Miner.* **1999**, *34*, 7–25. [CrossRef]
27. Négrel, P.; Sadeghi, M.; Ladenberger, A.; Reimann, C.; Birke, M. Geochemical fingerprinting and source discrimination of agricultural soils at continental scale. *Chem. Geol.* **2015**, *396*, 1–15. [CrossRef]
28. Liu, Z.; Wang, H.; Hantoro, W.S.; Sathiamurthy, E.; Colin, C.; Zhao, Y.; Li, J. Climatic and tectonic controls on chemical weathering in tropical Southeast Asia (Malay Peninsula, Borneo, and Sumatra). *Chem. Geol.* **2012**, *291*, 1–12. [CrossRef]
29. Singer, A. The paleoclimatic interpretation of clay minerals in soils and weathering profiles. *Earth Sci. Rev.* **1980**, *15*, 303–326. [CrossRef]
30. Chamley, H. *Clay Sedimentology*; Springer: Berlin/Heidelberg, Germany; New York, NY, USA, 1989; 623p.
31. Hu, B.; Li, J.; Cui, R.; Wei, H.; Zhao, J.; Li, G.; Fang, X.; Ding, X.; Zou, L.; Bai, F. Clay mineralogy of the riverine sediments of Hainan Island, South China Sea: Implications for weathering and provenance. *J. Asian Earth Sci.* **2014**, *96*, 84–92. [CrossRef]
32. Shanahan, T.M.; Pigati, J.S.; Dettman, D.L.; Quade, J. Isotopic variability in the aragonite shells of freshwater gastropods living in springs with nearly constant temperature and isotopic composition. *Geochim. Cosmochim. Acta* **2005**, *69*, 3949–3966. [CrossRef]
33. Li, H.C.; Ku, T.L. $\delta^{13}C$-$\delta^{18}O$ covariance as a paleohydrological indicator for closed-basin lakes. *Palaeogeogr. Palaeoclimatol. Palaeoecol.* **1997**, *133*, 69–80. [CrossRef]
34. Rowland, J.C.; Lepper, K.; Dietrich, W.E.; Wilson, C.J.; Sheldon, R. Tie channel sedimentation rates, oxbow formation age and channel migration rate from optically stimulated luminescence (OSL) analysis of floodplain deposits. *Earth Sur. Proc. Landf.* **2005**, *30*, 1161–1179. [CrossRef]
35. Hammarlund, D.; Björck, S.; Buchardt, B.; Israelson, C.; Thomsen, C. Rapid hydrological changes during the Holocene revealed by stable isotope records of lacustrine carbonates from Lake Igelsjön, southern Sweden. *Quart. Sci. Rev.* **2003**, *22*, 353–370. [CrossRef]